

Evidence for de Vries structure in a smectic-A liquid crystal observed by polarized Raman scattering

Naoki Hayashi* and Tatsuhisa Kato

*Institute for Molecular Science, Myodaiji, Okazaki 444-8585, Japan*Atsuo Fukuda, Jagdish K. Vij,[†] and Yuri P. Panarin*Department of Electronic and Electrical Engineering, Trinity College, University of Dublin, Dublin 2, Ireland*

J. Naciri and R. Shashidhar

Center for Bio/Molecular Science and Engineering, Naval Research Laboratory, Code 6900, 4555 Overlook Avenue South West, Washington, DC 20375, USA

Sachiko Kawada and Shinya Kondoh

Citizen Watch Co., Ltd., Tokorozawa 359-8511, Japan

(Received 3 September 2003; revised manuscript received 26 July 2004; published 25 April 2005)

The second- and fourth-order apparent orientational order parameters of the core part of the molecule $\langle P_2 \rangle_{\text{app}}$ and $\langle P_4 \rangle_{\text{app}}$, have been measured by polarized vibrational Raman spectroscopy for a homogeneously aligned ferroelectric smectic liquid crystal with three dimethyl siloxane groups in the achiral terminal chain, which shows de Vries-type phenomena, i.e., very large electroclinic effect in the smectic-A (Sm-A) phase and a negligible layer contraction at the phase transition between the Sm-A and Sm-C* phases. The apparent orientational order parameters of the rigid core part of the molecule are extremely small both with and without the external electric field in Sm-A. These results provide evidence for the existence of the de Vries Sm-A phase, where the local molecular director is tilted at a large angle.

DOI: 10.1103/PhysRevE.71.041705

PACS number(s): 61.30.Cz, 61.30.Gd, 64.70.Md

I. INTRODUCTION

The smectic-A (Sm-A) liquid crystal phase is constructed by piling two-dimensional layers in which the in-layer director \mathbf{n} is parallel to the layer normal. When the constituent liquid crystal molecule has chirality, an application of external electric field induces an average tilt of the molecules with respect to the layer normal. This phenomenon is known as the electroclinic effect [1]. Suppose that the smectic layer spacing is simply determined by the rigid molecular length, the tilting due to the electroclinic effect should cause the layer contraction by a factor of $\cos \theta$, where θ is the tilt angle between the in-layer director and the layer normal [2]. This layer contraction is observed as stripes parallel to the layer normal in homogeneously aligned sandwich cells [3] and these stripes are found to be detrimental to the working of a good display.

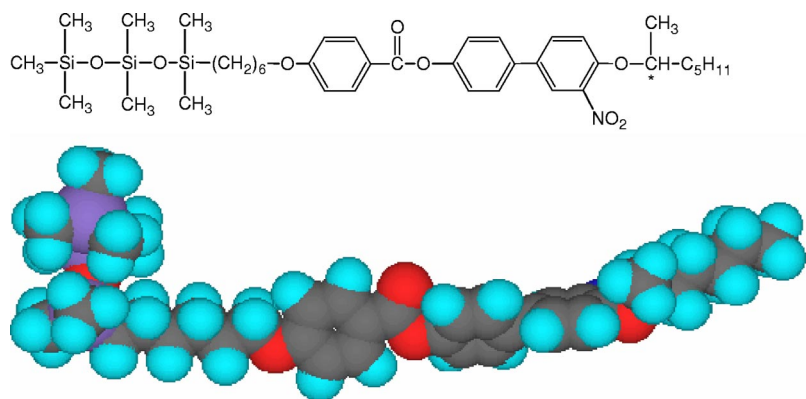
In some chiral smectic liquid crystals however, the molecules tilt but the layers do not contract [4]. These materials have a large potential for useful applications in displays and devices. This behavior can occur as a function of decreasing temperature into the smectic-C* (Sm-C*) phase, or under an applied electric field in the smectic-A phase. Adrien de Vries studied this behavior in nonchiral smectics only [5–7], and

suggested that it is caused by a disordered molecular orientation in the smectic-A phase, which becomes more ordered under decreasing temperature or increasing electric field. Since then, liquid crystals exhibiting this behavior are generally called de Vries materials and a class of materials involving chiral smectics have recently gained importance due to their potential for applications in photonic devices. Selinger *et al.* [8] have reported the results of experiments of tilt angle and birefringence of DSiKN65 and TSiKN65 with one and two siloxane spacer(s) and have concluded that these materials have a disordered distribution of molecular tilt directions that is aligned by the electric field. This is found to be the basis of the large electroclinic effect. Recently several other groups [9–14] investigated this behavior using x-ray diffraction and electro-optical studies of such chiral smectics. Their results are consistent with the de Vries concept that the molecular orientation is initially disordered but becomes more ordered under an applied electric field. However, the limitation of those experiments is that they provide only indirect information about the orientational ordering of the molecules.

In this paper, we go beyond those earlier experiments by using polarized Raman scattering to study one of these materials. The technique of polarized Raman scattering provides direct measurements of the second $\langle P_2 \rangle$ and the fourth order $\langle P_4 \rangle$ orientational order parameters of the liquid-crystal molecules. We denote the experimentally measured values by a subscript “app” which implies that these are apparent order parameters which are generally different from the molecular orientational order parameters. Our experiments show that

*Present address: Advanced Core Laboratory, Fuji Photo Film Co., 210 Nakanuma, Minami-Ashigara, Kanagawa 250-0193, Japan. Electronic address: naoki_a_hayashi@fujifilm.co.jp

[†]Electronic address: jvij@tcd.ie



SmC* - 25 °C – SmA* – 56 °C – Is

$\langle P_2 \rangle_{\text{app}}$ is low under zero electric field, and increases under an applied field. This result is consistent with the de Vries concept, and with the earlier measurements using other techniques. Our experiments also show that $\langle P_4 \rangle_{\text{app}}$ is very low with or without an applied electric field. This result shows that the molecular core has a large tilt with respect to the molecular long axis.

These chiral smectics in general show a large electroclinic effect with a small or without a measurable layer contraction [9–15]. They do have a large potential for applications to fast response electro-optic devices because no defects due to the layer contraction may appear during the switching process. These materials may have disordered azimuthal angles of the molecular directors, when the transition to Sm-C* occurs, the azimuths align into one direction and sense. Hence the layer spacing is kept constant while the average local directors tilts with respect to the layer normal at the same time. The apparent orientational ordering of molecular long axes in Sm-C* becomes higher than in de Vries Sm-A. The long molecular axis is defined such that it gives rise to the lowest moment of inertia for the molecule. We introduce the term “in-layer director” as already mentioned in the beginning of the Introduction. In this context the “in-layer director” is defined as the director of a swarm of molecules with the same azimuthal angle. The azimuthal angle may vary within the layer as well as from layer to layer. What really exists or is possible in a chiral smectic, which exhibits large electroclinic effect and a small or unmeasurable layer shrinkage at the Sm-A to Sm-C* transition, is beyond the scope of this paper.

The material under study (TSiKN65) synthesized by Naciri *et al.* was found to have significantly large electroclinic effect [8,15] and exhibits a small layer contraction in the Sm-A phase even when a large electric field is applied across the cell [11] as well as from Sm-A to Sm-C* phase in the absence of a field. The experimental results obtained by using dissolved dichroic dyes [14] and infrared spectroscopy [10] show that the orientational order parameter is indeed found to be very small compared to that obtained for conventional Sm-A or Sm-C* even when a large electric field is applied across the cell. However, the origin of the small orientational order parameters is not understood because no detailed direct information about the local molecular structure has so far been reported in the literature.

FIG. 1. (Color online) Chemical structure, molecular shape and phase sequence of a liquid crystal 4-[3'-nitro-4'-(R)-1-methylhexyloxy] phenyl 4-(6-heptylmethyltrisiloxy-hexyloxy) benzoate (TSiKN65).

II. EXPERIMENT

The chemical structure of a smectic liquid crystal synthesized by Naciri *et al.* [15] and used here is shown in Fig. 1. A homogeneously aligned sandwich cell was prepared. The material is introduced between the two quartz glass substrates coated with indium tin oxide using the capillary effect. These ITO coated substrates were spin coated with ~20-nm-thick polyimide (Nissan, RN-1266) aligning films and only one of them was rubbed in one direction and sense, since this material may also show the very large interface-induced electroclinic effect [16–18]. The gap of the cell was set at 2.5 μm by the ball spacers. A well-aligned sample was obtained through a rapid cooling from the isotropic to Sm-A without applying any electric field (Fig. 2). There are still many small defects visible in the texture, and hence scattering was observed from a well-aligned uniform area by using a micro-Raman spectrometer, Renishaw RM1000. An argon ion laser was used for the excitation source. The wavelength was fixed to be 514.5 nm and the power was set at 30 mW. The diameter of the focused spot was less than 3 μm . The magnification of the objective lens was 20. The sample cell was mounted in a temperature-controlled oven that is attached to a rotational stage. Polarized and depolarized spectra were measured as a function of the rotation angle of the cell from 0° to 180° in order to evaluate the orientational order parameters.

III. RESULTS

Figure 3 shows the polarized Raman spectra obtained in the isotropic phase at 65 °C. Three Raman lines were analyzed for evaluating the orientational order parameters. These are assigned to the C-C stretching vibration of nitrophenyl (line 1, 1604 cm^{-1}), the C-C stretching vibration of phenyl (line 2, 1620 cm^{-1}), and the C-O stretching vibration of core part carbonyl (line 3, 1733 cm^{-1}) groups of the molecule. The longest principal axes of the Raman tensors for these lines are known to lie almost parallel to the long axis of the core part of the molecule [19,20]. The depolarization ratios in the isotropic phase $R_{\text{iso}} = I_{\perp} / I_{\parallel}$, are listed in Table I, where I_{\parallel} and I_{\perp} are the polarized and depolarized intensities. The overlapped Raman lines are deconvoluted by assuming

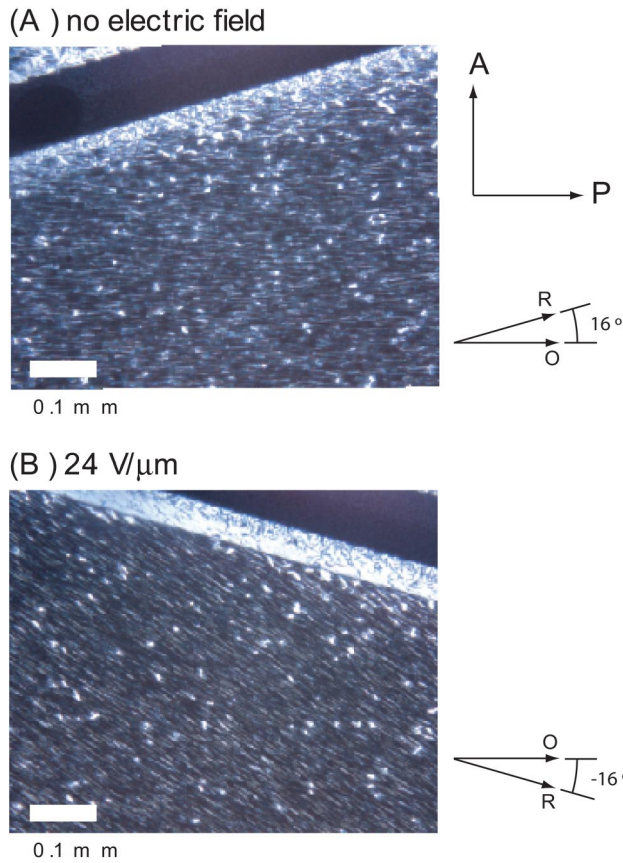


FIG. 2. (Color online) Optical micrographs observed by polarizing microscope at 30 °C (a) without any electric field and (b) with an applied electric field of 24 V/μm. The analyzer and polarizer are parallel to the vertical and horizontal edges of the photograph, respectively. The edge of the sample is parallel to the rubbing direction, which is indicated by arrow R. The optical axis is parallel to the horizontal line of the photograph, which is indicated by arrow O. The white bar at the left bottom of the photograph represents the length of 0.1 mm. Only the lower substrate is rubbed and the field is directed from lower to upper.

the Lorentzian shape and I_{\parallel} 's and I_{\perp} 's are obtained by integrating the fitted Lorentzian curves.

For a homogeneously aligned cell in a liquid crystal phase, the depolarization ratio of the polarized Raman intensity $R(\omega) = I_{\perp}(\omega)/I_{\parallel}(\omega)$ varies with the rotation angle of the cell ω . Figures 4(a) and 4(b) are the polar plots of $1/R(\omega)$ profiles as a function of ω obtained at a temperature of 30 °C in the Sm-A phase in the absence of electric field ($E=0$ V/μm) and on the application of a high electric field ($E=24$ V/μm), respectively. The maximum point of $1/R(\omega)$ profile indicates the average orientation of the longest principal axis of the Raman tensor. The average orientations for three Raman lines investigated here are parallel to the layer normal for $E=0$ V/μm while these tilt by 32° at $E=24$ V/μm. The electric field of 24 V/μm was found to almost saturate the tilt angle [10]. The polarizing microscope observation confirms that the apparent molecular tilt angle is 32° as shown in Fig. 2. The shapes of $1/R(\omega)$ at $E=24$ V/μm is found to be clearly different from those at

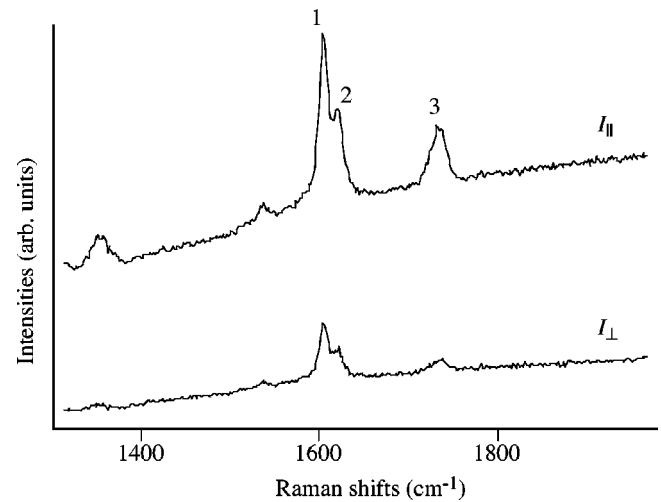


FIG. 3. Polarized Raman spectra I_{\parallel} and I_{\perp} measured at 65 °C in the isotropic phase.

$E=0$ V/μm; this indicates a change in the orientational order of the molecules.

The fitting procedure described in a previous paper [21] gives results for the second- and fourth-order apparent orientational order parameters $\langle P_2 \rangle_{\text{app}}$ and $\langle P_4 \rangle_{\text{app}}$, for the longest principal axis of the Raman tensor with respect to the averaged orientational direction [19–23], as summarized in Table I. Note that the uniaxial Raman scattering tensor is assumed in obtaining values for $\langle P_2 \rangle_{\text{app}}$ and $\langle P_4 \rangle_{\text{app}}$. Since the longest principal axis is parallel to the long axis of the core part, $\langle P_2 \rangle_{\text{app}}$ and $\langle P_4 \rangle_{\text{app}}$ given in Table I represent the apparent orientational order parameters for the core part of the molecule. Experimentally, only small differences in $\langle P_2 \rangle_{\text{app}}$ and $\langle P_4 \rangle_{\text{app}}$ among the three Raman lines are observed here. When no electric field is applied, $\langle P_2 \rangle_{\text{app}}$ and $\langle P_4 \rangle_{\text{app}}$ are extremely small and these are found to be almost independent of temperature. The very small values of $\langle P_2 \rangle_{\text{app}}$ have

TABLE I. Depolarization ratios R_{iso} and apparent orientational order parameters $\langle P_2 \rangle_{\text{app}}$ and $\langle P_4 \rangle_{\text{app}}$, obtained by polarized Raman scattering measurements. The depolarization ratio was measured in the isotropic phase at 65 °C.

	line 1 (1604 cm ⁻¹)	line 2 (1620 cm ⁻¹)	line 3 (1733 cm ⁻¹)
R_{iso}	0.453	0.413	0.255
	0 V/μm at 30 °C		
$\langle P_2 \rangle_{\text{app}}$	0.30±0.02	0.27±0.02	0.28±0.02
$\langle P_4 \rangle_{\text{app}}$	-0.05±0.02	0.00±0.03	-0.06±0.03
	0 V/μm at 50 °C		
$\langle P_2 \rangle_{\text{app}}$	0.26±0.01	0.27±0.01	0.25±0.02
$\langle P_4 \rangle_{\text{app}}$	-0.04±0.01	0.01±0.02	-0.11±0.03
	24 V/μm at 30 °C		
$\langle P_2 \rangle_{\text{app}}$	0.48±0.05	0.44±0.06	0.51±0.05
$\langle P_4 \rangle_{\text{app}}$	0.12±0.04	0.13±0.04	0.07±0.06

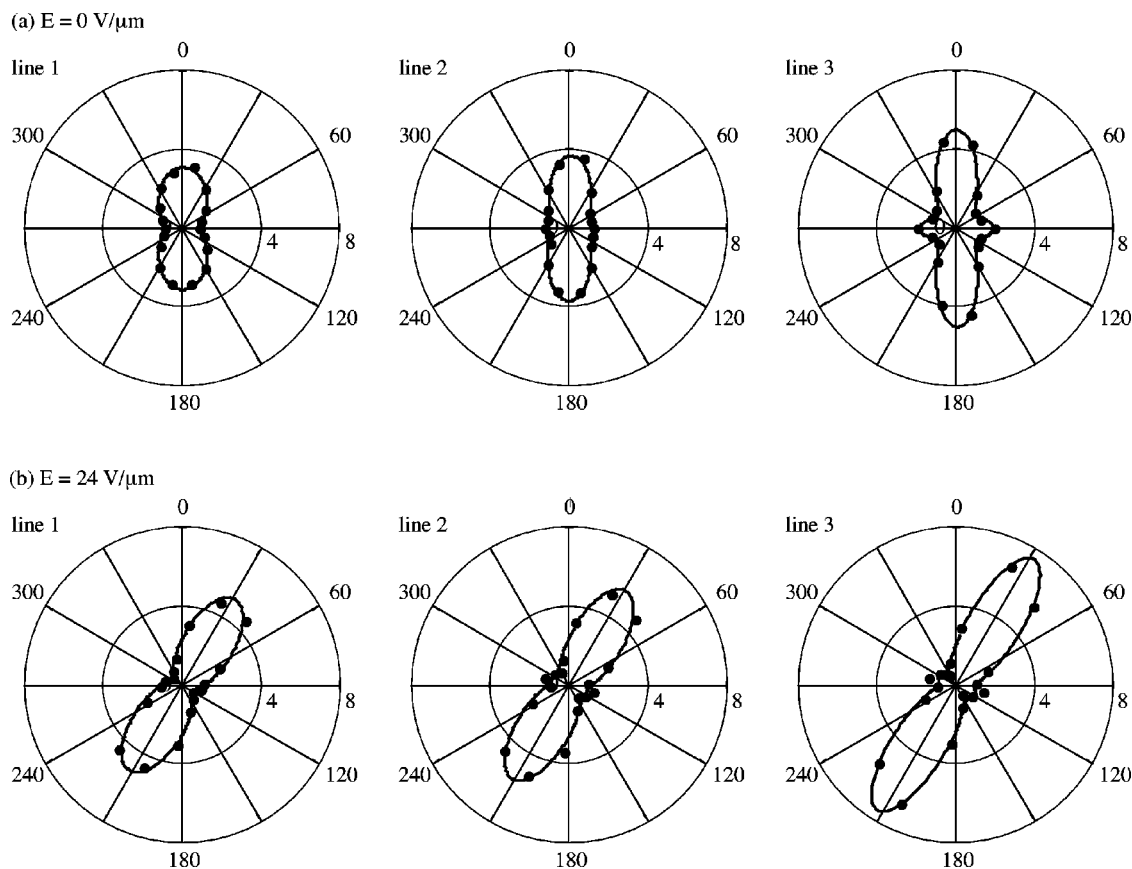


FIG. 4. Polar plots of reciprocal values of the depolarization ratio $R(\omega)=I_{\perp}(\omega)/I_{\parallel}(\omega)$ at 30 °C, where ω is the rotation angle (deg.) of the sample cell: (a) $E=0$ and (b) $E=24$ V/ μ m. Solid circles are experimental values and solid lines are the theoretically fitted curves. The line connecting between 0° and 180° shows the direction parallel to the smectic layer normal.

also been pointed out in the previous works [10,14]. It is remarkable that $\langle P_4 \rangle_{app}$ values are approximately zero, and those calculated for the lines 1 and 3 show even negative values. At a temperature of 30 °C, the electric field of 24 V/ μ m almost saturates the tilt angle as mentioned before [10]. Under this high electric field, values for $\langle P_2 \rangle_{app}$ and $\langle P_4 \rangle_{app}$ are increased. Nevertheless, the orientational order parameters still remain very small and the value of $\langle P_4 \rangle_{app}$ is approximately only 0.1.

IV. DISCUSSION

A. Relation between the apparent and the molecular orientational order parameters

To interpret the extremely small apparent orientational order parameters correctly, the relation between the experimentally obtained “apparent” orientational order parameters $\langle P_2 \rangle_{app}$ and $\langle P_4 \rangle_{app}$, and the “molecular” orientational order parameters $\langle P_2 \rangle$ and $\langle P_4 \rangle$, must be considered. Since the longest principal axis of the Raman tensor possibly tilts somewhat with respect to the molecular long axis as shown in Fig. 5(a), $\langle P_2 \rangle_{app}$ and $\langle P_4 \rangle_{app}$ may generally differ from $\langle P_2 \rangle$ and $\langle P_4 \rangle$ even in an orthogonal Sm-A phase. Therefore, $\langle P_2 \rangle_{app}$ and $\langle P_4 \rangle_{app}$ depend not only on the molecular thermal fluctuations but also on the angle β_0 between the longest

principal axis of the Raman tensor and the molecular long axis [19,20]. Since the longest principal axes of the Raman tensors for the lines used are almost parallel to the long axis of the core part of the molecule as pointed out previously and especially detailed in Ref. [20], β_0 is assumed to be equal to the tilt angle of the core part with respect to the molecular long axis, β_C . Moreover, we have to take into account the distribution of the local in-layer directors in the de Vries scenario.

When the molecular orientational distribution function $f(\beta)$ has uniaxial symmetry, where the symmetry axis is parallel to the in-layer director, $f(\beta)$ is described by an expansion expressed in terms of the Legendre polynomials

$$f(\beta) = \sum_{L=even} \frac{2L+1}{8\pi^2} \langle P_L \rangle P_L(\cos \beta), \quad L = 2 \text{ and } 4. \quad (1)$$

Here the angle β is the tilt angle. The second- and fourth-order “molecular” orientational order parameters $\langle P_2 \rangle$ and $\langle P_4 \rangle$ are given by

$$\langle P_L \rangle = \frac{\int_0^\pi \sin \beta d\beta P_L(\cos \beta) f(\beta)}{\int_0^\pi \sin \beta d\beta f(\beta)}, \quad L = 2 \text{ and } 4. \quad (2)$$

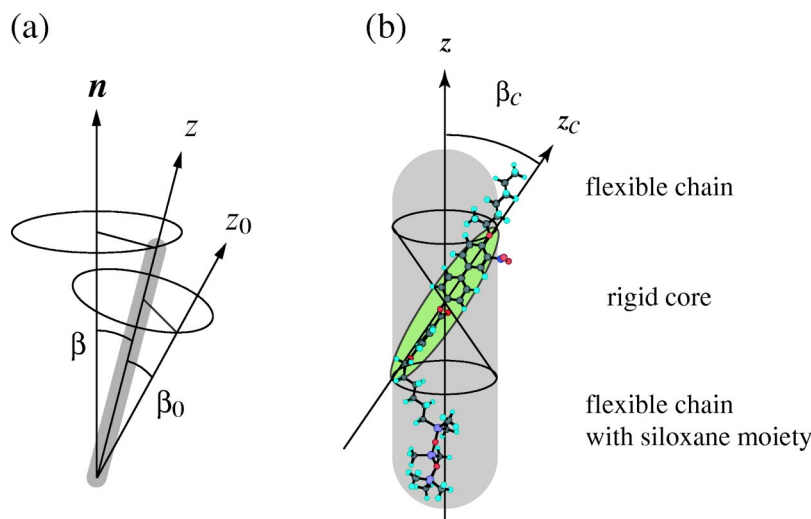


FIG. 5. (Color online) Schematic illustrations representing (a) the molecular long axis is defined such that it gives the lowest moment of inertia (the z axis), the averaged direction of the molecular long axes (the in-layer director \mathbf{n}), and the longest principal axis of the Raman tensor (the z_0 axis), and (b) the molecular long axis (the z axis) and the long axis of the core part (the z_c axis) when the core part is assumed to be a rigid rod with a uniaxial symmetry. β is the molecular tilt angle at an instant of time, β_0 the angle between the z and z_0 axes, and β_c the angle between the z and z_c axes. The molecular orientational distribution has uniaxial symmetry around their long axes, of which the distribution around the in-layer director is uniaxial. The z_c and z_0 axes are almost parallel to each other and hence we assume $\beta_0 = \beta_c$ in this paper. The conformation of the chemical structure illustrated may not be real but is drawn just for the ease of understanding.

Here $P_2(\cos \beta)$ and $P_4(\cos \beta)$ are the second- and fourth-order Legendre polynomials. These order parameters are not explicitly dependent on the azimuthal angle of the director. We define the direction z to be the molecular long axis such that the moment of inertia of the molecule across which is the least. We define the direction z_c as the long axis of the core part; the angle β_c as the angle between z and z_c . The experimentally obtained “apparent” orientational order parameters $\langle P_2 \rangle_{\text{app}}$ and $\langle P_4 \rangle_{\text{app}}$, may still not be given by Eq. (2) if $\beta_c \neq 0$ since the apparent order parameters are measured relative to the layer normal; these are related to the “molecular” orientational order parameters $\langle P_2 \rangle$ and $\langle P_4 \rangle$, as follows [21,22]:

$$\langle P_L \rangle_{\text{app}} = P_L(\cos \beta_c) \langle P_L \rangle, \quad L = 2 \text{ and } 4. \quad (3)$$

Here, we assume the uniaxial molecular orientational distribution around the director though the orientational distribution in the field induced ferroelectric state is really biaxial [20,21] and hence this representation as $\langle P_L \rangle$ is only approximate and is based on the assumption that the molecular rotational bias in general is practically rather small ($\sim 10\text{--}15\%$) [24]. The influence of the biaxiality on the results obtained will be discussed in the Sec. IV B. Note that the rotational bias would only affect the value of the tilt angle that is calculated (Sec. IV B), it should have no influence at all on the measured value of the orientational order parameter (Sec. IV C).

In a usual Sm-A phase, the in-layer directors are parallel to the smectic layer normal in the absence of the electric field, the fluctuations of which must be small and negligible. The apparent orientational order parameters $\langle P_2 \rangle_{\text{app},0}$ and $\langle P_4 \rangle_{\text{app},0}$, are given by

$$\langle P_L \rangle_{\text{app},0} = P_L(\cos \beta_c) \langle P_L \rangle_0, \quad L = 2 \text{ and } 4. \quad (4)$$

When an electric field is applied, the average molecular tilt is induced due to the electroclinic effect. Since the in-layer directors tilt with respect to the layer normal uniformly, the apparent orientational order parameters under sufficiently large electric field $\langle P_2 \rangle_{\text{app},E}$ and $\langle P_4 \rangle_{\text{app},E}$ are given by

$$\langle P_L \rangle_{\text{app},E} = P_L(\cos \beta_c) \langle P_L \rangle_E, \quad L = 2 \text{ and } 4. \quad (5)$$

In de Vries Sm-A, the local in-layer directors (director of the region over which the order is smectic C-like) tilt with respect to the layer normal and randomly distribute on the tilt cone as shown in Fig. 6(a). The apparent order parameters $\langle P_2 \rangle_{\text{app},0}$ and $\langle P_4 \rangle_{\text{app},0}$, are given in terms of the average of the molecular orientational distribution in a single layer over all azimuthal tilt orientations

$$\langle P_L \rangle_{\text{app},0} = P_L(\cos \theta) P_L(\cos \beta_c) \langle P_L \rangle_0, \quad L = 2 \text{ and } 4, \quad (6)$$

where θ is the tilt angle of the local in-layer director with respect to the smectic layer normal. In field-induced tilted Sm-C*, all the in-layer directors are oriented in one direction and sense as illustrated in Fig. 6(b). Since there is no spatial distribution of the in-layer directors as shown in Fig. 6(b), the orientational order parameters under high electric field $\langle P_2 \rangle_{\text{app},E}$ and $\langle P_4 \rangle_{\text{app},E}$ are given by Eq. (5). The origin of the extremely small apparent orientational order parameters listed in Table I is discussed in terms of Eqs. (3)–(6) as follows.

B. Possible interpretations of a small molecular order parameter

The orientational order parameters in electric-field-induced tilted Sm-C* are examined first. In this state, the

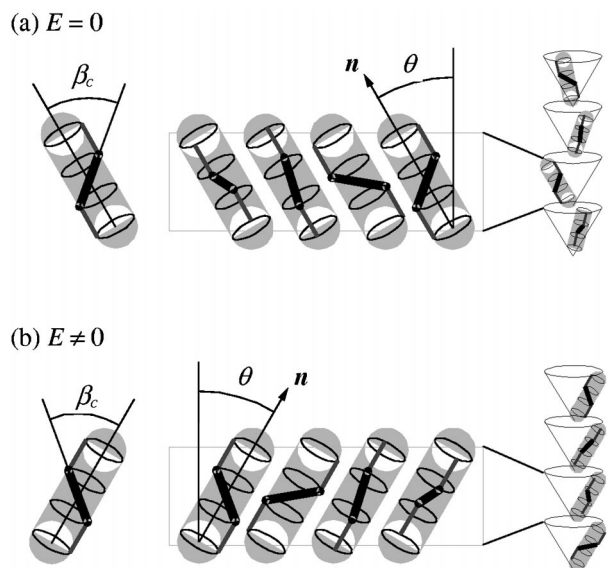


FIG. 6. Scenario based on de Vries Sm-A: (a) de Vries Sm-A phase in the absence of applied electric field, where the local in-layer directors tilt with respect to the layer normal by θ and randomly distribute on the Sm-C* tilt cone even in a single layer as well from layer to layer and (b) the electric field-induced tilted Sm-C* phase, where the local in-layer directors align in the same direction and sense so that the tilt plane is perpendicular to the applied field, keeping the tilt angle θ to be a constant. Note that, as already explained in Fig. 5, the longest axis of the core part (the z_C axis) tilts relative to the molecular long axis (the z axis) by angle β_C .

in-layer directors are oriented in one direction and sense as illustrated in Fig. 6(b). Consider two possible cases, which can interpret such a small orientational order parameters in terms of Eq. (5).

The first interpretation could have easily been that $\langle P_2 \rangle_E$ and $\langle P_4 \rangle_E$ do have very small values due to the microscopic segregation between the siloxane part on the terminal chain and the molecular core part on the basis of the x-ray and dilatometry measurements in analogous liquid crystals containing the siloxane group [25]. However, the assumption of the low molecular orientational order may be questioned because the observed large electroclinic effect does indicate a large spontaneous polarization. This inevitably requires high molecular orientational order parameter. Such a large spontaneous polarization as already mentioned is actually observed for an analogous series of materials [14].

The second interpretation is based on the molecular structure of this compound: a highly noncalamitic molecular shape with a largely tilted core part. Note that the compound, which has the same core part but no siloxane substituent in the terminal chain (KN125, [15]), shows a typical value of the orientational order parameter. The modeling by semi-empirical molecular orbital calculation suggested the presence of a large angle between the core part of the molecule and the average molecular long axis [11], i.e., β_C . Hence $P_2(\cos \beta_C)$ and $P_4(\cos \beta_C)$ may have very small values due to a large β_C . It is natural to consider that $\langle P_2 \rangle_E$ and $\langle P_4 \rangle_E$ have typical values in the smectic phase under the suffi-

ciently large electric field. Since $\langle P_4 \rangle_{app,E}$ is as low as 0.1, $P_4(\cos \beta_C)$ should be close to 0. Hence β_C should be close to the magic angle for the fourth-order Legendre polynomial $\beta_C = 30.5^\circ$, for $P_4(\cos \beta_C) = 0$. When $\langle P_2 \rangle_E = 0.7$ and $\langle P_4 \rangle_E = 0.5$ are assumed as the typical values, we obtain $\beta_C = 26^\circ$, $\langle P_2 \rangle_{app,E} = 0.50$ and $\langle P_4 \rangle_{app,E} = 0.10$ by using Eq. (5). Similarly, when $\langle P_2 \rangle_E = 0.8$, and $\langle P_4 \rangle_E = 0.6$ are assumed, we obtain $\beta_C = 28.5^\circ$, $\langle P_2 \rangle_{app,E} = 0.53$, and $\langle P_4 \rangle_{app,E} = 0.05$. In this way, large β_C is deduced for all Raman lines that have been investigated here. However, it should be noted that the deduced values of β_C are based on Eq. (3), the validity of which is being investigated here for the case of a real biaxial system. These values would be found to be even slightly higher when large biaxiality is considered than the angle found for a uniaxial case.

It is possible to estimate the influence of biaxiality on Eq. (3). For this estimation, we assume Gaussian distribution of the molecular short axis

$$f(\phi) = \frac{1}{4\pi\sqrt{2\pi}\sigma} \exp\left[-\frac{(\phi - \phi_0)^2}{2\sigma^2}\right], \quad (7)$$

where ϕ is the angle between the molecular short axis and the axis parallel to the tilt plane. The latter is parallel to the substrates when E is applied. The molecular short axis lies in the molecular tilt plane. ϕ_0 is the angle around which the short axis is distributed. When the electric field is applied to the sample cell, the in-layer director also parallel to the substrate plates and $\phi_0 = 0$. $\sigma = 0$ corresponds to the perfect orientation of the molecular short axis and thus the maximal biaxiality. For this $|\langle \cos(\phi - \phi_0) \rangle| = 1$ and $\sigma = 0$. In a uniaxial case, $|\langle \cos(\phi - \phi_0) \rangle| = 0$ and $\sigma = \infty$. The biaxiality may be found using Eq. (8):

$$\begin{aligned} \langle \cos(\phi) \rangle &= \int_0^{2\pi} \frac{1}{4\pi\sqrt{2\pi}\sigma} \exp\left[-\frac{(\phi - \phi_0)^2}{2\sigma^2}\right] \\ &\times \cos \phi d\phi \bigg/ \int_0^{2\pi} \frac{1}{4\pi\sqrt{2\pi}\sigma} \\ &\times \exp\left[-\frac{(\phi - \phi_0)^2}{2\sigma^2}\right] d\phi. \end{aligned} \quad (8)$$

The spontaneous polarization is proportional to $\langle \cos(\phi) \rangle$. Next we want to find the effect of the biaxiality on the simulated values of the apparent order parameters $\langle P_2 \rangle$ and $\langle P_4 \rangle$. Let us assume that $\langle P_2 \rangle_E = 0.8$ and $\langle P_4 \rangle_E = 0.6$ as the actual values of the molecular order parameters for a complete biaxial case, and the core tilt angle as $\beta_C = 28.5^\circ$.

The apparent order parameters are simulated by assuming the biased distribution of the azimuthal angle of the core part around the long molecular axis. For the uniaxial case, $\sigma = \infty$ [for which Eq. (3) is strictly valid] the apparent order parameters as simulated are found to be $\langle P_2 \rangle_{app,E} = 0.53$ and $\langle P_4 \rangle_{app,E} = 0.05$. For the case of a 15% biaxiality $\langle \cos(\phi - \phi_0) \rangle = 0.15$ and $\sigma = 140^\circ$, the order parameters as simulated are found to be $\langle P_2 \rangle_{app,E} = 0.54$ and $\langle P_4 \rangle_{app,E} = 0.10$. These simulated values are approximately the same as those obtained for the uniaxial case. A comparison of the order pa-

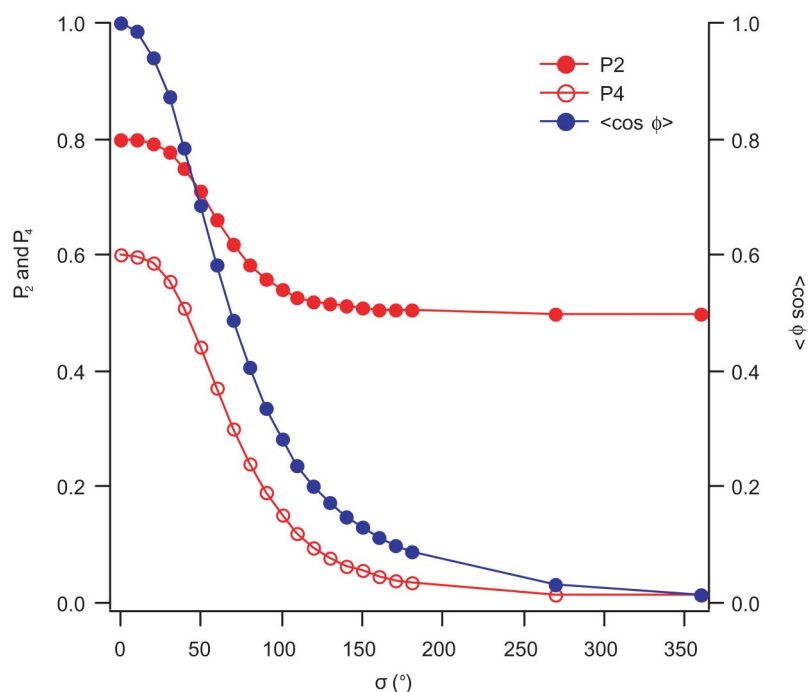


FIG. 7. (Color online) Simulated values of $\langle P_2 \rangle_{\text{app},E}$ and $\langle P_4 \rangle_{\text{app},E}$ for $\beta_C = 30^\circ$ as a function of σ (deg). For $\sigma = 0^\circ$, assumed values of $\langle P_2 \rangle_E$ and $\langle P_4 \rangle_E$ are 0.8 and 0.6, respectively. Procedure of simulation is given in Ref. [21], except here the core is tilted with respect to the in-layer direction, whereas in Ref. [21], the molecule is tilted with respect to the layer normal.

rameters for these two cases: the uniaxial and for a limited biaxial case, shows that the Eq. (3) derived for a uniaxial case is also valid for the case of a limited biaxiality. However, we can simulate the orientational order parameters for any degree of biaxiality and indirectly calculate the angle β_C . This core tilt angle would increase with the increase in the biaxiality. The procedure for simulation of the order parameters is detailed by Hayashi *et al.* [21] in Sec. V of their paper. The simulations are carried out as a function of σ and are shown in Fig. 7. Due to a competition between the privileged direction of the transverse dipole moment close to the chiral carbon atom and the almost free rotation of the molecule around its long molecular axis, the biaxiality in most compounds in Sm-C* is found to be of the order of 10–20% [26].

Hence the extremely small “apparent” orientational order parameters can be understood in terms of the core part of the molecule having been largely tilted with respect to the molecular long axis [Fig. 5(b)]. This interpretation reasonably accounts the experimental observation of the small “apparent” orientational order parameters or it may also be supplemental to the mechanism already given by Collings *et al.* [14].

C. de Vries Sm-A or usual Sm-A?

The observation of the small apparent orientational order parameters in the absence of the externally applied electric field can be explained in terms of the de Vries scenario as follows. Application of a sufficiently large electric field of $24 \text{ V}/\mu\text{m}$ makes the in-layer directors align in one direction and sense perpendicular to the applied field and the field-induced tilted state is identical to the Sm-C* phase [Fig. 6(b)] [10]. It can be assumed that the “molecular” orientational order parameters $\langle P_2 \rangle$ and $\langle P_4 \rangle$ are independent of the strength of the applied electric field

$$\langle P_L \rangle = \langle P_L \rangle_0 = \langle P_L \rangle_E, \quad L = 2 \text{ and } 4. \quad (9)$$

According to Eqs. (5)–(7), the L th order “apparent” orientational order parameter in the absence of the electric field $\langle P_L \rangle_{\text{app},0}$ is related to $\langle P_L \rangle_{\text{app},E}$ with

$$\langle P_L \rangle_{\text{app},0} = P_L(\cos \theta) \langle P_L \rangle_{\text{app},E}. \quad (10)$$

As shown in Table I and Figs. 2 and 4, $\theta = 32^\circ$, $\langle P_2 \rangle_{\text{app},E} = 0.48$ and $\langle P_4 \rangle_{\text{app},E} = 0.12$ are obtained for line 1 at $24 \text{ V}/\mu\text{m}$. Equation (10) gives $\langle P_2 \rangle_{\text{app},0} = 0.28$ and $\langle P_4 \rangle_{\text{app},0} = -0.01$ for the de Vries Sm-A phase. These simulated values approximate the experimentally obtained values in the absence of the external electric field. The de Vries scenario can thus explain not only the results obtained by the Raman experiment but can also offer explanation for the results of the other experiments reported previously [10,11,14].

The molecular weight of the rigid terminal chain containing siloxane substituent (Fig. 1), is calculated to be $\sim 2/5$ of the entire molecule, the molecular structure possesses a highly noncalamitic overall molecular shape. This may cause a disturbance in the long-range ordering of the molecules in smectic layers and therefore may lead to the formation of the de Vries structure as was indeed earlier pointed out by Selinger *et al.* [8] through their experimental and theoretical works. The Monte Carlo simulation method also shows that the “bent-rod” shaped molecular structure, found in this study, causes the molecular tilt with respect to smectic layer normal and makes the vortexlike point defects [27], which appear in the modulated phase. Recently, Meyer and Pelcovits [28] theoretically proposed the existence of a modulated Sm-C* phase for the de Vries Sm-A phase. The local in-layer n directors in a smectic layer tilt relative to the layer normal and these are azimuthally disordered on the tilt cone even in a single layer though some correlation of the azimuthal direction may exist in the adjacent layers, thus forming an

array of vortices or defects. If the spacing of these defects were to appear in the subvisible region, this modulated Sm-C* phase would look similar to a Sm-A phase. No direct experimental verification of this theoretical proposal has yet been reported to our knowledge.

V. CONCLUSION

The apparent second- and fourth-order orientational order parameters are investigated for the ferroelectric liquid crystal showing the so-called de Vries-type Sm-A phase using the polarized Raman spectroscopy. Extremely low orientational order parameters have experimentally been obtained even when a large external electric field that produces the director tilt angle as large as 32° is applied across the cell. The analysis of these results indicates that the core part is largely tilted with respect to the long molecular axis. The model calculations based on Eq. (3) shown here to be valid for a biaxiality of $\sim 15\%$, lead to the result that the tilt angle of the core is of the order of 26° – 36° . It is also shown that at least in principle, the tilt angle of the core part can be estimated for any degree of biaxiality since the order parameters for any degree

of biaxiality can be simulated. The change in the apparent orientational order parameters between the states with the externally applied electric field is discussed in terms of de Vries Sm-A scenario. The analysis of the results of the experiments using polarized Raman spectroscopy provides an evidence for the existence of de Vries Sm-A phase in the siloxane material investigated here.

ACKNOWLEDGMENTS

The authors thank Nissan Chemical Industries, Ltd., for supplying the aligning material. The Raman scattering experimental part of the work was carried out in Trinity College Dublin (TCD) for which T.S. Perova is acknowledged for introducing us to the spectrometer. J.K.V thanks the Science Foundation, Ireland (SFI) [02/IN.1/I031] for supporting the visit of N.H. to Dublin and for funding the research. Atsuo Fukuda also thanks the SFI [02/W/I02] for financial support at Trinity College Dublin. We sincerely thank Dr. Jonathan V. Selinger for informal discussions about the de Vries type of materials. One of the authors (J.K.V.) thanks R. Korlacki for discussions on IR spectroscopy.

-
- [1] S. Garoff and R. B. Meyer, *Phys. Rev. Lett.* **38**, 848 (1977).
 - [2] There are several counter examples indicating the inappropriateness of this assumption. See, e.g., Y. Takanishi, H. Takezoe, and A. Fukuda, *Ferroelectrics* **147**, 135 (1993).
 - [3] J. Pavel and M. Glogarova, *Ferroelectrics* **114**, 131 (1991).
 - [4] B. R. Ratna, R. Shashidhar, G. G. Nair, S. K. Prasad, C. Bahr, and G. Heppke, *Phys. Rev. A* **37**, 1824 (1988).
 - [5] A. de Vries, *Mol. Cryst. Liq. Cryst.* **41**, 27 (1977).
 - [6] A. de Vries, A. Ekachai, and N. Spielberg, *Mol. Cryst. Liq. Cryst.* **49**, 143 (1979).
 - [7] A. de Vries, *Mol. Cryst. Liq. Cryst.* **49**, 179 (1979).
 - [8] J. V. Selinger, P. J. Collings, and R. Shashidhar, *Phys. Rev. E* **64**, 061705 (2001).
 - [9] F. Giesselmann, P. Zugenmaier, I. Dierking, S. T. Lagerwall, B. Stebler, M. Kaspar, V. Hamplova, and M. Glogarova, *Phys. Rev. E* **60**, 598 (1999).
 - [10] O. E. Panarina, Yu. P. Panarin, J. K. Vij, M. S. Spector, and R. Shashidhar, *Phys. Rev. E* **67**, 051709 (2003).
 - [11] M. S. Spector, P. A. Heiney, J. Naciri, B. T. Weslowski, D. B. Holt, and R. Shashidhar, *Phys. Rev. E* **61**, 1579 (2000).
 - [12] J. P. F. Lagerwall, F. Giesselmann, and M. D. Radcliffe, *Phys. Rev. E* **66**, 031703 (2002).
 - [13] N. A. Clark, T. Bellini, R.-F. Shao, D. Coleman, S. Bardon, D. R. Link, J. E. MacLennan, X.-H. Chen, M. D. Wand, D. M. Walba, P. Rudquist, and S. T. Lagerwall, *Appl. Phys. Lett.* **80**, 4097 (2002).
 - [14] P. J. Collings, B. R. Ratna, and R. Shashidhar, *Phys. Rev. E* **67**, 021705 (2003).
 - [15] J. Naciri, J. Ruth, G. Crawford, R. Shashidhar, and B. R. Ratna, *Chem. Mater.* **7**, 1397 (1995).
 - [16] K. Nakagawa, T. Shinomiya, M. Kodan, K. Tsubota, T. Kuratate, Y. Ishii, F. Fukuda, M. Matsuura, and K. Awane, *Ferroelectrics* **85**, 39 (1988).
 - [17] J. S. Patel, S.-D. Lee, and J. W. Goodby, *Phys. Rev. Lett.* **66**, 1890 (1991).
 - [18] W. Chen, Y. Ouchi, T. Moses, Y. R. Shen, and K. H. Yang, *Phys. Rev. Lett.* **68**, 1547 (1992).
 - [19] S. Jen, N. A. Clark, P. S. Pershan, and E. B. Priestley, *J. Chem. Phys.* **66**, 4635 (1977).
 - [20] N. Hayashi and T. Kato, *Phys. Rev. E* **63**, 021706 (2001).
 - [21] N. Hayashi, T. Kato, T. Aoki, T. Ando, A. Fukuda, and S. S. Seomun, *Phys. Rev. E* **65**, 041714 (2002).
 - [22] N. Hayashi, T. Kato, T. Ando, and A. Fukuda, *Jpn. J. Appl. Phys., Part 1* **41**, 5292 (2002).
 - [23] N. Hayashi, T. Kato, T. Ando, A. Fukuda, S. Kawada, and S. Kondoh, *Phys. Rev. E* **68**, 011702 (2003).
 - [24] A. A. Sigarev, J. K. Vij, R. A. Lewis, M. Hird, and J. W. Goodby, *Phys. Rev. E* **68**, 031707 (2003).
 - [25] E. Corsellis, D. Guillon, P. Kloess, and H. J. Coles, *Liq. Cryst.* **23**, 235 (1997).
 - [26] A. Kocot, J. K. Vij, and T. S. Perova, in *Advances in Liquid Crystals*, edited by J. K. Vij (Wiley, New York, 2000), printed in a special issue of *Adv. Chem. Phys.* **113**, 203 (2000).
 - [27] J. Xu, R. L. B. Selinger, J. V. Selinger, B. R. Ratna, and R. Shashidhar, *Phys. Rev. E* **60**, 5584 (1999).
 - [28] R. B. Meyer and R. A. Pelcovits, *Phys. Rev. E* **65**, 061704 (2002).